PCCP

PAPER

View Article Online
View Journal | View Issue

Cite this: *Phys. Chem. Chem. Phys.*, 2017, **19**, 17044

Efficient scavenging of Criegee intermediates on water by surface-active *cis*-pinonic acid†

Shinichi Enami *[a] and A. J. Colussi *[b]

Received 4th April 2017,
Accepted 14th June 2017

DOI: 10.1039/c7cp03869k

rsc.li/pccp

cis-Pinonic acid (CPA), the main product of the atmospheric oxidation of biogenic α-pinene emissions and a major component of secondary organic aerosol (SOA), is a potentially key species *en route* to extremely low volatility compounds. Here, we report that CPA is an exceptionally efficient scavenger of Criegee intermediates (CIs) on aqueous surfaces. Against expectations, millimolar CPA (a surface-active C_{10} keto-carboxylic acid possessing a rigid skeleton) is able to compete with 23 M bulk water for the CIs produced in the ozonolysis of sesquiterpene solutes by O_3(g) on the surface of a water:acetonitrile solvent. The significance of this finding is that CPA reactions with sesquiterpene CIs on the surface of aqueous organic aerosols would directly generate C_{25} species. The finding that competitive reactions at the air–liquid interface depend on interfacial rather than bulk reactant concentrations should be incorporated in current chemical models dealing with SOA formation, growth and aging.

Introduction

Ozonolysis of olefins is a major source of Criegee intermediates (CIs)[1] in the atmosphere. CIs are extremely reactive carbonyl oxide ($R_2C{=}O^+{-}O^-$) intermediates that participate in HOx cycling and particle formation.[2–11] Recent experiments have revealed that olefins may not only be processed in the gas-phase, but can be reactively uptaken *via* protonation on the surface of acidic aqueous aerosols.[12–16] Olefins thereby trapped may react with O_3(g) to generate CIs *in situ*.[17,18] Previously, we had found that the heterogeneous ozonolysis of β-caryophyllene (a major biogenic sesquiterpene) by O_3(g) on the surface of water proceeds ~20 times faster and by a different mechanism than in bulk water saturated with O_3(g) at the same partial pressure.[19] The fate of CIs generated on the surface of realistic aqueous aerosols containing other organic species, however, is not known.

Theoretical calculations have predicted that the reaction of the simplest CI: $H_2C{=}O^+{-}O^-$, with water proceeds much faster at the air–water interface than in the gas-phase *via* an interface-specific mechanism.[20] We recently found that *n*-alkyl carboxylic acids R_n-COOH (n = 1–7) compete (their competitiveness increasing with n) with interfacial water molecules for CIs in the outermost interfacial layers of water/acetonitrile mixtures.[21] This finding is the most remarkable because, against all expectations, it indicates that surface-active acids in the millimolar range of are able to compete with a large excess of water molecules. This observation was ascribed to the combined effects of the low water concentrations prevalent in the outermost interfacial layers, and the enrichment of the more hydrophobic, longer alkyl-chain acids therein. This phenomenon bears directly on aerosol accretion and growth because CIs, by reacting with organics rather than water at the interface, lead directly to the formation larger, low volatility molecules *via* a process that has not hitherto been considered in chemical models of organic aerosol formation. In this paper we extend our studies and show that *cis*-pinonic acid (CPA), a surface-active[22] ubiquitous byproduct of terpenes gas-phase oxidation and a major component of secondary organic aerosol (SOA), is a singularly effective scavenger of CIs on aqueous organic surfaces.

CPA, the most common acid produced from massive biogenic volatile organic compound (BVOC) emissions, is largely generated in the gas-phase *via* α-pinene reactions with O_3 and the OH-radical.[23–27] Some CPA remains in the gas-phase, some will condense on preexisting dry aerosols and the rest will partition to aqueous aerosols (Henry's law constant: $H \sim 2 \times 10^7$ M atm^{-1}) (Scheme 1).[24,28] In fact, CPA is a major component of ultrafine particles over boreal forests.[29] Field measurements of CPA concentrations in particulate matter report values ranging from 10^{-7} to 10^{-8} g m^{-3}, which are comparable to those of oxalic acid, the most abundant carboxylic acid in aerosols everywhere.[25,30–32] In this paper, we demonstrate that bulk CPA concentrations do not fully capture its potential reactivity in the outermost interfacial layers due to its large surface affinity, as revealed by molecular dynamics (MD) calculations, surface-tension data

[a] *National Institute for Environmental Studies, 16-2 Onogawa, Tsukuba, Ibaraki 305-8506, Japan. E-mail: enami.shinichi@nies.go.jp; Tel: +81-29-850-2770*
[b] *Linde Center for Global Environmental Science, California Institute of Technology, California 91125, USA. E-mail: ajcoluss@caltech.edu; Tel: +1-626-395-6350*

† Electronic supplementary information (ESI) available: Additional experimental data. See DOI: 10.1039/c7cp03869k

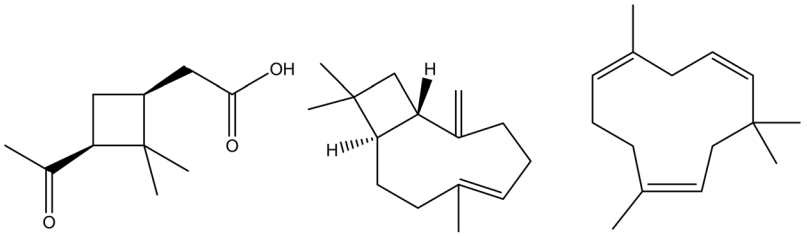

***cis*-pinonic acid (CPA)**
Chemical Formula: $C_{10}H_{16}O_3$
Molecular Weight: 184.23

β-caryophyllene (β-C)
Chemical Formula: $C_{15}H_{24}$
Molecular Weight: 204.35

α-humulene (α-H)
Chemical Formula: $C_{15}H_{24}$
Molecular Weight: 204.35

Scheme 1 Chemical structures of the reactant species used in the present study.

and surface-sensitive mass spectrometry.[33–37] A molecular dynamics study has predicted that all 144 CPA molecules partition to the interfacial layers of a $(H_2O)_{2000}$ droplet, confirming the exceptional affinity of CPA for the air–water interface.[33] Experiments employing interface-specific mass spectrometry have shown that *cis*-pinonate has a significantly larger affinity than *n*-octanoate for the air–water interface.[37] The surface enrichment of CPA will enhance its participation in interfacial reactions in condensed-phase aqueous media.

Here we report the first detection of intermediates and products from CPA reactions with CIs generated on fresh surfaces of β-caryophyllene (β-C) and α-humulene (α-H) solutions in acetonitrile (AN):water (W) exposed to O_3(g) for ∼10 μs. Sesquiterpenes are chosen as *in situ* CIs sources due to their high reactivities toward O_3(g),[19] which make them compatible with the short $\tau_R \sim 10$ μs contact times in our experiments.[38–40] We utilize a AN:W mixture solvent as a surrogate of atmospheric aqueous organic media because the composition of its interfacial layers is well characterized both by theory and experiments.[41,42] Our results suggest CPA is a major scavenger of the CIs produced from ozonolysis of BVOCs on aqueous organic aerosols.

Methods

The present experimental setup is essentially the same as those we reported elsewhere.[21,43] We utilize a mixture of sesquiterpene + *cis*-pinonic acid in AN : W (4 : 1 = vol : vol) microjets into the spraying chamber of an electrospray mass spectrometer (ES-MS, Agilent 6130 Quadrupole LC/MS Electrospray System at NIES, Japan) flushed with N_2(g) at 1 atm, 298 K. Microjets are exposed therein to orthogonal gas-phase O_3/O_2 beam (Fig. 1).

These mass spectra correspond to species generated by heterogeneous processes in the outermost (≤1 nm) interfacial layers of the intact injected microjets, as repeatedly confirmed by a series of experiments in our laboratory involving diverse chemistries.[38,39,43–45] The relatively small ozone exposures: $E = [O_3(g)] \times \tau_R \leq 2.4 \times 10^{11}$ molecules cm^{-3} s, used in our experiments enables us to probe the hitherto inaccessible early stages of alkene ozonations on liquid surfaces. AN:W solutions containing β-C, CPA and NaCl were pumped (100 μL min^{-1}) into the spraying chamber through a grounded stainless steel needle (100 μm bore) coaxial with a sheath issuing nebulizer

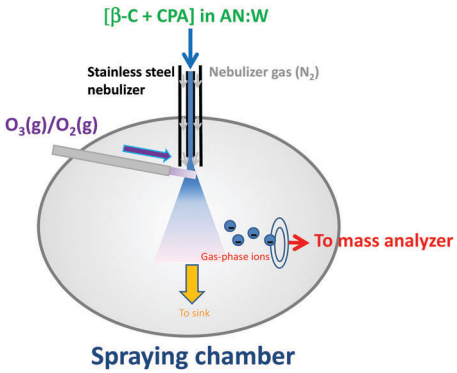

Fig. 1 Schematic diagram of the present experimental setup.

N_2(g) at a high gas velocity v_g (∼160 m s^{-1}).[46] Neutral species were detected as negatively charged chloride-adducts displaying characteristic M/M + 2 = 3/1 signal intensities arising from natural abundance ^{35}Cl/^{37}Cl isotopes. We previously verified that chloride is inert towards O_3(g) under present conditions, as expected from $k_{O_3+Cl^-} < 0.003$ M^{-1} s^{-1} in bulk water.[47,48] Online, *in situ* sampling of the outermost interfacial layers of continually refreshed aqueous microjets at ambient temperature and pressure makes our experimental setup a valuable surface-sensitive technique.[49,50] Further experimental details could be found in previous publications.[21,37,39,40,43,45,46]

Ozone was generated by flowing ultrapure O_2(g) (>99.999%) through a silent discharge ozonizer (KSQ-050, Kotohira, Japan) and quantified *via* online UV-vis absorption spectrophotometry (Agilent 8453) at 300 nm where σ (300 nm) = 3.9×10^{-19} cm^2 molecule^{-1} at 298 K prior to entering the reaction chamber. The reported [O_3(g)] values correspond to the concentrations actually sensed by the microjets in the reaction chamber that are estimated to be ∼12 times smaller than the values determined from UV absorbance due to dilution by the drying nitrogen gas. Conditions in the present experiments were: drying nitrogen gas flow rate: 12 L min^{-1}; drying nitrogen gas temperature: 340 °C; inlet voltage: +3.5 kV relative to ground; fragmentor voltage value: 60 V. All solutions were prepared in purified water (resistivity ≥18.2 M cm at 298 K) from a Millipore Milli-Q water purification system and used within a couple of days. All data were confirmed by at least duplicate experiments. Chemicals: β-caryophyllene (≥98.5%, Sigma-Aldrich), α-humulene (≥96.0%, Sigma-Aldrich),

cis-pinonic acid (≥98%, Sigma-Aldrich), octanoic acid (>97%, Wako), acetonitrile (≥99.8%, Wako), D_2O (>99.9 atom% D, Sigma-Aldrich) and NaCl (≥99.999%, Sigma-Aldrich) were used as received.

Results and discussion

Fig. 2 shows negative ion electrospray mass spectrum of 1 mM β-C + 0.2 mM NaCl + 1 mM CPA in AN : W (4 : 1 = vol : vol) solution microjets in the absence and presence of O_3(g). CPA (MW 184, pK_a = 4.8)[51] exists both as pinonate (CPA^-, *m*/*z* 183) and neutral CPA, which is detected as its chloride-adduct at *m*/*z* = 184 + 35 (37) = 219 (221) (Fig. 2A). Minor signals at *m*/*z* 241 (and 243) and 389 are assigned to $NaCl(CPA)^-$ and $Na(CPA)_2^-$ clusters, respectively (Fig. 2B). By lacking C=C bonds, both CPA and CPA^- proved to be inert toward O_3(g) in the absence of β-C.[37]

In the presence of O_3(g), intense peaks appear at *m*/*z* 305/307 and 471/473 in the M/(M + 2) = 3/1 = $^{35}Cl/^{37}Cl$ ratio (Fig. 2A). The *m*/*z* 305/307 signals are readily assigned to species resulting from the addition of O_3 (+48) to a β-C (MW = 204) endo C=C bond,[10,19] followed by H_2O addition (+18), which are detected as chloride-adducts: 305 (307) = 204 + 48 + 18 + 35 (37).[21] Our observation that neutral hydroxy-hydroperoxides form stable, detectable chloride-adducts is in line with previous reports on chloride affinity for related species.[7,52,53] As mentioned above, we had previously shown that the ozonolysis of β-C on AN:W surfaces proceeds ~20 times faster than in the bulk liquid saturated with ozone,[19] and orders of magnitude faster than in the gas-phase.[10,54] The *m*/*z* 471/473 corresponds to the products of CPA addition to CIs: 471 (473) = 204 + 48 + 184 + 35 (37) (Scheme 2).

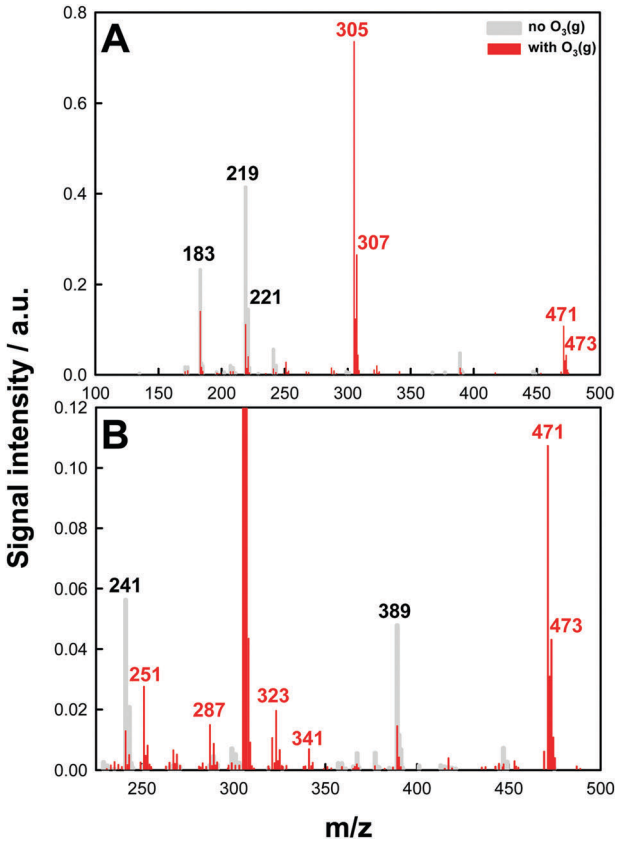

Fig. 2 (A) Negative ion electrospray mass spectra of 1 mM β-caryophyllene + 0.2 mM NaCl + 1 mM *cis*-pinonic acid in AN : W (4 : 1 = vol : vol) solution microjets (gray), or those exposed to O_3(g) (red, E = 1.4 × 10^{11} molecules cm^{-3} s) at 1 atm and 298 K. (B) Zooming in spectra of the products in the 230–500 Da range. The *m*/*z* 305/307 and 471/473 signals correspond to chloride-adducts of α-hydroxy-hydroperoxides and α-acyloxy-hydroperoxides (C_{25} species), respectively. See the text for details.

Hence, the *m*/*z* 471/473 signals are assigned to the α-acyloxy-hydroperoxides (C_{25} ester species) produced from the reaction of CIs with CPA (see below). We recently found that 100 mM *n*-alkyl carboxylic acids R_n-COOH ($n \geq 4$) compete with interfacial water molecules for β-C or α-H CIs on the surface of AN:W.[21] In the present case, we find that 1 mM CPA is already able to compete with interfacial water for CIs to generate a high mass product (MW 436, detected as *m*/*z* 471 and 473) instead of the *m*/*z* = 305 α-hydroxy-hydroperoxides from CI reaction with $(H_2O)_n$. This finding reveals that CPA, a C_{10} keto-carboxylic acid possessing a rigid hydrophobic backbone, is a more effective scavenger than alkanoic acids of similar size at the air–aqueous interface. The behavior of α-humulene is similar to that of β-C: intense peaks at *m*/*z* 305/307 and 471/473 appear in the ozonolysis of a mixture of α-H + CPA in AN:W microjets (Fig. S1, ESI†). The implication is that sesquiterpene CIs generated *in situ* will generally react with CPA on aqueous organic surfaces under typical atmospheric conditions.[31,55–57]

The formation of α-acyloxy-hydroperoxides is consistent with previous reports on ozonolyses in bulk condensed-phase.[26,58–62] Recently, high molecular mass species were observed as major products in aerosols produced in the laboratory *via* α-pinene ozonolysis, as well as in fresh aerosols collected over boreal forests.[63] Such studies, however, did not fully provide the mechanisms underlying their observations. Our results suggest the involvement of *interfacial* CIs chemistry in the prompt generation of molecular complexity. As noted above, since both BVOCs and BVOC-acids are naturally surface-active, their interfacial chemistry will contribute to the formation of larger mass products. Since thermally and photochemically labile α-hydroxy-hydroperoxides and α-acyloxy-hydroperoxides are more reactive than their β-C and CPA precursors, they will likely trigger radical polymerization processes furthering chemical complexity (see below).[3,28,64,65]

The enhanced reactivity of CPA towards CIs relative to alkanoic acids of similar molecular complexity may be accounted by its peculiar molecular geometry (see below).[33,37] Lacking an active C(O)–OH group, CPA^- anions do not react with CIs, as revealed by the absence of signals at *m*/*z* 435 that would have arisen from: 435 = 204 + 48 + 183. Other anionic species at *m*/*z* 251 and 287/289 formally arise from the addition of three O-atoms to β-C, which corresponds to functionalized-carboxylate anions detected as such (*m*/*z* = 251 = 204 + 48 − 1) or as chloride-adducts of secondary ozonides (*m*/*z* = 287 (289) = 204 + 48 + 35 (37)), respectively.[19,21] The smaller signal intensities of these species (including *m*/*z* 323 and

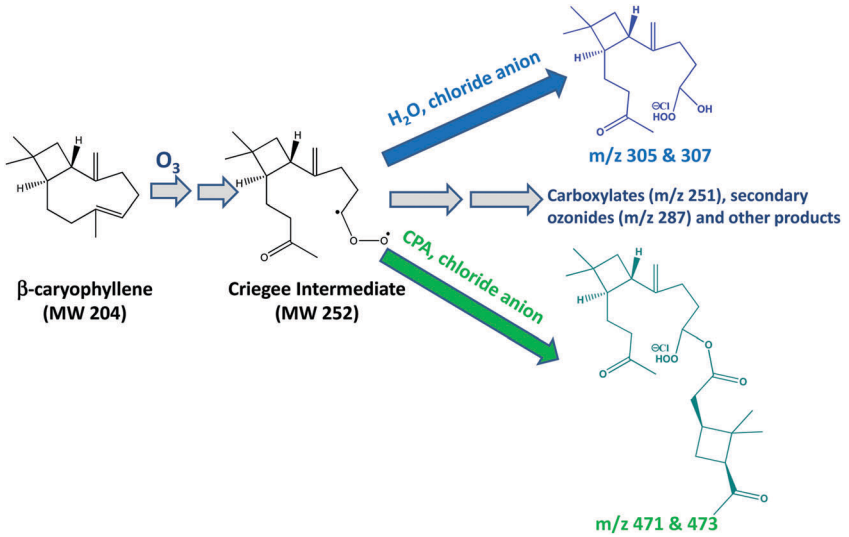

Scheme 2 Reaction scheme of β-caryophyllene's Criegee intermediate + *cis*-pinonic acid at air–aqueous interfaces. Here we show representative structures among possible isomers.

341) relative to those at *m*/*z* 305 and 471, suggest they are products of a minor reaction channel. These minor products may have similar structures to those reported for the interfacial α-H ozonolysis (Fig. S1, ESI†).[21] The presence of exo and endo double bonds in β-C may lead to numerous isomers and conformers. The characterization of their molecular structures, however, falls outside the scope of the present study, which aims at elucidating the mechanism of generation of chemical complexity in the early stages of SOA growth and aging. High-resolution MS/MS analyses and theoretical calculations could assist in making structural assignments.

Fig. 3 shows negative ion electrospray mass spectrum of 1 mM β-C + 0.9 mM NaCl + 10 mM CPA in AN : D_2O (4 : 1 = vol : vol) solution microjets in the absence and presence of O_3(g). Chloride–CPA adduct signals at *m*/*z* 219 (and 221) in AN:W (Fig. 2A) shift to *m*/*z* 220 (and 222) in AN:D_2O (Fig. 3), as expected. The *m*/*z* = 305/307 product signals shift by +2 mass units into 307/309 signals in AN:D_2O (Fig. 3), as expected from α-hydroxy-hydroperoxides having exchangeable alcohol –O(H) and hydroperoxide –OO(H) H-atoms (Scheme 2).[21] The *m*/*z* = 471/473 product signals shift by +1 mass units into 472/474 signals in AN:D_2O (Fig. 3), consistent with the formation of α-acyloxy-hydroperoxides having a single exchangeable –OOH group. These results support the proposed ketone rather than aldehydic functionalities in the detected α-hydroxy-hydroperoxides and α-acyloxy-hydroperoxides (Scheme 2).

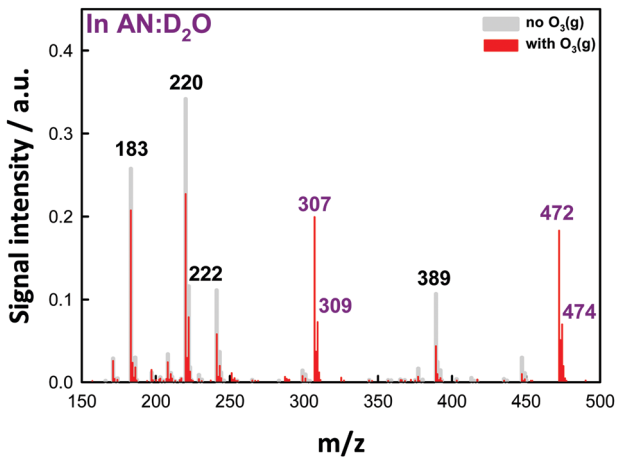

Fig. 3 Negative ion electrospray mass spectra of 1 mM β-caryophyllene + 0.9 mM NaCl + 10 mM *cis*-pinonic acid in AN : D_2O (4 : 1 = vol : vol) solution microjets (gray), or those exposed to O_3(g) (red, E = 2.3 × 10^{11} molecules cm^{-3} s) at 1 atm and 298 K.

Fig. 4 shows electrospray mass spectral signals acquired from 1 mM β-C + 0.2 mM NaCl in AN : W (4 : 1 = vol : vol) microjets with 1 mM and 20 mM CPA exposed to gaseous O_3/O_2 mixtures as functions of O_3(g) exposure. All signals display non-zero initial slopes, implying that these are early products generated within a few microseconds. The largest *m*/*z* = 305 (and 307) signals at low [CPA] (Fig. 4A) peak at $E \sim 7 \times 10^{10}$ molecules cm^{-3} s and decline afterward, which is consistent with further O_3 addition to the remaining exo-double bond or, more likely, to unpaired electrons as predicted by theoretical calculations.[66,67] The decline of *m*/*z* = 305 (and 307) signals above $E \sim 7 \times 10^{10}$ molecules cm^{-3} s implies that at large O_3(g) exposures these species are depleted faster than being produced. The implication is that β-C is partially depleted in the interfacial layers probed by our experiments, indicating that the β-C + O_3 reaction is faster than β-C diffusion from the bulk solution into interfacial layers under present conditions.

The *m*/*z* = 471 signals are much smaller than the *m*/*z* = 305 in 1 mM CPA (Fig. 4A), while the formation of *m*/*z* = 471 exceeds over *m*/*z* 305 in 20 mM CPA (Fig. 4C). In the latter case, in contrast with [CPA] = 1 mM experiments, both *m*/*z* = 305 and 471 signals increase with E to plateau above $E > 2.4 \times 10^{11}$ molecules cm^{-3} s (Fig. 4C). This is ascribed to the fact

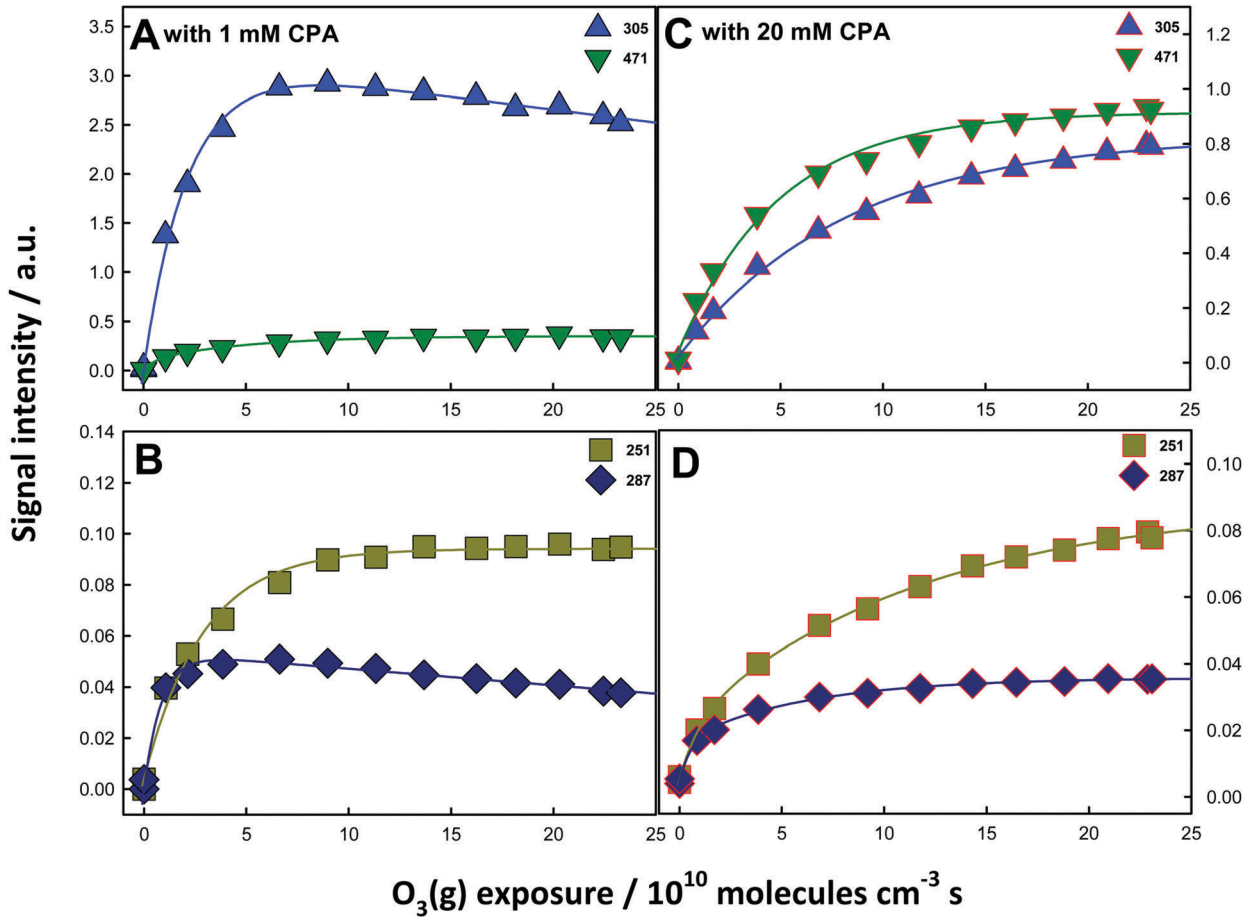

Fig. 4 Products mass spectral signal intensities from 1 mM β-caryophyllene + 0.2 mM NaCl + 1 mM (A and B) and 20 mM (C and D) *cis*-pinonic acid in AN : W (4 : 1 = vol : vol) solution microjets exposed to O_3(g) as functions of O_3(g) exposure (in 10^{10} molecules cm^{-3} s). The lines are regression curves fitted with single and double exponential growth functions.

that strongly surface-active CPA,[33,37,55] which is inert toward O_3,[37] begins to displace β-C from the surface at [CPA] ≥ 20 mM. Similar shielding effects by surfactants have been reported previously.[68–71] The minor *m*/*z* = 251 and 287 signals are also influenced by CPA (Fig. 4B and D). The key finding is that CIs react equally fast with CPA and interfacial H_2O at bulk concentration ratios: [CPA]/[H_2O] = 20 mM/23 M ∼ 10^{-3} (molar fraction of H_2O = 0.42 in 4 : 1::AN : W). The key notion that CPA and water reactivities at the air–liquid interface are dictated by their interfacial rather than bulk concentrations should be incorporated in the conceptual framework of chemical mechanisms dealing with aerosol formation, growth and aging.

The competition between CPA and water at the gas–liquid interface at constant O_3 exposure is quantified by the 471/305 ratio as a function of CPA concentration (Fig. 5). The saturation-like behavior observed in Fig. 5 is consistent with a surface that becomes increasingly populated by amphiphilic CPA, which reacts with CIs but is inert toward O_3. The fact that the *m*/*z* 471 signal intensity increases while that at *m*/*z* 305 monotonically decreases as a function of [CPA] (Fig. S2, ESI†) implies that CPA replaces both $(H_2O)_n$ and hydrophobic β-C at the surface. Our findings suggest that CIs reactions take place in interfacial layers where water concentration is a very small

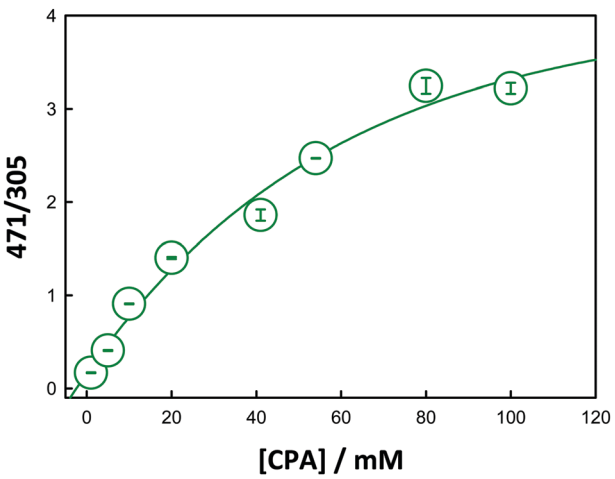

Fig. 5 The ratio of signal intensity at *m*/*z* 471 to *m*/*z* 305 as a function of concentration of added *cis*-pinonic acid to 1 mM β-caryophyllene + 0.2 mM NaCl in AN : H_2O (4 : 1 = vol : vol) solution microjets in the presence of O_3 (E = 2.4 × 10^{11} molecules cm^{-3} s). The line is an exponential growth fitting. Error bars were derived from 2–3 independent experiments. See text for details.

fraction of its bulk value.[37,72–74] This is consistent with recent theoretical and experimental studies which have shown that

above AN ~ 0.2 molar fraction, the air–liquid interface of AW/W mixtures consists of a compact AN layer, which likely extends to the second layer.[41,42]

Notably, we could not see anionic products that would have resulted from CIs addition to β-C. The absence of such products is in line with the relatively small gas-phase rate constants for CIs + olefins (typical $k_{CIs+C=C} \leq 10^{-13}$ cm^3 molecule^{-1} s^{-1}) predicted by theoretical calculations,[66] *vis-á-vis* the collisionally controlled ($k_{CIs+RCOOH} \sim 10^{-10}$ cm^3 molecule^{-1} s^{-1}) gas-phase reactions of CH_2OO/CH_3CHOO with formic/acetic acids.[75] Theoretical calculations revealed that steric hindrance slows down CIs reactions with bulky alkenes by up to 4 kcal mol^{-1} barriers.[66] The same study shows that steric hindrance induces pronounced regio- and stereo-selectivity effects on CIs reactions with alkenes,[66] suggesting that the relative orientations of CIs and reactants at the interface could further modulate CIs reactivities and selectivities at the air–liquid interface.

These effects are illustrated by the competition between CPA *vs.* octanoic acids towards CIs. Fig. 6 shows negative ion electrospray mass spectra of 1 mM β-C + 0.2 mM NaCl + 10 mM CPA + 10 mM octanoic acid (OA, MW 144) in AN : W (4 : 1 = vol : vol) solution microjets in the absence or presence of O_3(g). The peaks at *m*/*z* 431 and 433 correspond to the products of OA addition to CIs: 431 (433) = 204 + 48 + 144 + 35 (37).[21] We previously found that OA is inert toward O_3(g) under present conditions.[45] The observation that signal intensities at *m*/*z* 431 (and 433) are ~5 times smaller than *m*/*z* 471 (and 473) at [CPA] = [OA] = 10 mM is another indication that CPA is more reactive than OA towards CIs because its molecular structure positions its active C(O)OH group nearer than OA to the air–water interface where CIs are generated.[37] CPA likely lies flat on the surface exposing its hydrophobic cyclobutane-ring to air, and keeping the hydrophilic carbonyl –C(O)– and the reactive carboxylic –C(O)OH groups lying immediately below,[33] in contrast with OA, whose –C(O)OH is likely buried deeper in bulk water at the end of its (long) alkyl chain. This observation suggests that CPA may be more reactive than other surface-active BVOC-acids due to its peculiar molecular geometry,[33,37] rather than to intrinsically larger surface affinity.

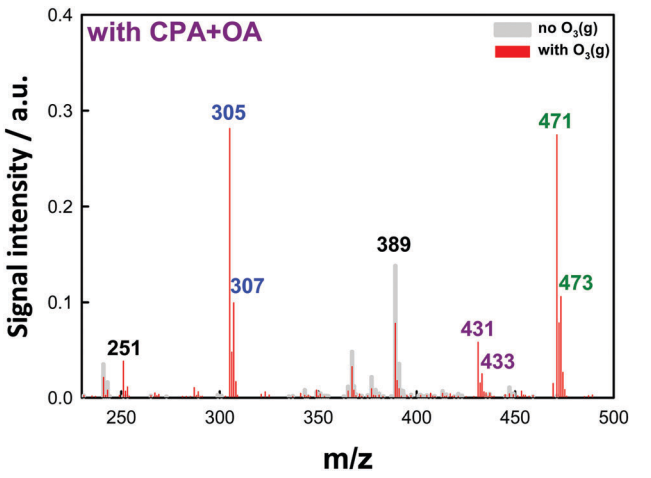

Fig. 6 Negative ion electrospray mass spectra of 1 mM β-caryophyllene + 0.2 mM NaCl + 10 mM *cis*-pinonic acid + 10 mM octanoic acid in AN : W (4 : 1 = vol : vol) solution microjets (gray), or those exposed to O_3(g) (red, $E = 2.3 \times 10^{11}$ molecules cm^{-3} s) at 1 atm and 298 K.

Our study is consistent with extremely fast heterogeneous ozonolyses in which O_3(g) initially sticks to the surface of aqueous organic aerosols to subsequently react with alkene BVOC and BVOC-acids. This process generates thermalized CIs that engage in bimolecular reactions, rather than undergoing unimolecular decomposition, leading to large mass products *via* unanticipated chemistry at the gas–liquid interface. As mentioned above, since CPA is a major component of ultrafine particles over boreal forests,[29] our experiments point to a major role of CPA in the development of molecular complexity in aqueous organic aerosols. Note that C_{25} products (MW 436, detected as *m*/*z* 471 and 473) have one (for β-C) and two (for α-H) remaining C=C double bond(s). Hence, they will undergo further ozonolysis at the interface leading to high O/C products.[21] Acyloxy –C(O)O– and hydroperoxide –OOH groups could undergo thermal, metal-catalyzed and photochemical decompositions into acyl, acyloxy and OH-radicals,[64,65] which propagate oligomerizations.[3,7,76] Such processes provide effective routes for the formation of the exceedingly low-volatility organic compounds (ELVOCs) recently found in field studies.[62,63,77,78] Chemical modeling studies will be required to fully elucidate the impact of our findings on atmospheric chemistry. We anticipate that present results will narrow the gap between field observations and model calculations that consistently underestimate SOA yields and O/C ratios.[77,79]

Conclusion

Our experiments show, for the first time, that Criegee intermediates produced by ozonolysis of sesquiterpenes preferentially react with surface-active *cis*-pinonic acid in the interfacial layers of model aqueous organic aerosols. We provide mass-specific direct identification of the products and intermediates in a very short (<10 μs) reaction time frames. Present results suggest that Criegee intermediates efficiently react with CPA rather than linear alkyl organic acids of similar size, or interfacial water molecules at air–aqueous interfaces. This phenomenon is ascribed to peculiar molecular geometry of CPA that positions the reactive –C(O)–OH group close to the interface. Such an interface-specific reaction mechanism has not been previously considered in chemical models of SOA formation. The facts that CPA is abundant in ambient particles, a very efficient scavenger of the CIs produced on aqueous organic surfaces, and a precursor of less volatile species, make CPA a major contributor to the formation and growth of atmospheric particles. The present results could narrow the current gap between field observations and atmospheric model calculations.

Author contributions

S. E. designed and performed research; S. E. and A. J. C. analyzed data and wrote the paper.

Acknowledgements

This work is partly supported by the research foundation for opto-science and technology, JSPS KAKENHI grant numbers 15H05328 and 15K12188.

References

1 R. Criegee, *Angew. Chem., Int. Ed. Engl.*, 1975, **14**, 745–752.
2 S. Hatakeyama and H. Akimoto, *Res. Chem. Intermed.*, 1994, **20**, 503–524.
3 Y. Sakamoto, R. Yajima, S. Inomata and J. Hirokawa, *Phys. Chem. Chem. Phys.*, 2017, **19**, 3165–3175.
4 T. B. Nguyen, G. S. Tyndall, J. D. Crounse, A. P. Teng, K. H. Bates, R. H. Schwantes, M. M. Coggon, L. Zhang, P. Feiner, D. O. Milller, K. M. Skog, J. C. Rivera-Rios, M. Dorris, K. F. Olson, A. Koss, R. J. Wild, S. S. Brown, A. H. Goldstein, J. A. de Gouw, W. H. Brune, F. N. Keutsch, J. H. Seinfeld and P. O. Wennberg, *Phys. Chem. Chem. Phys.*, 2016, **18**, 10241–10254.
5 L. Yao, Y. Ma, L. Wang, J. Zheng, A. Khalizov, M. D. Chen, Y. Y. Zhou, L. Qi and F. P. Cui, *Atmos. Environ.*, 2014, **94**, 448–457.
6 C. A. Taatjes, D. E. Shallcross and C. J. Percival, *Phys. Chem. Chem. Phys.*, 2014, **16**, 1704–1718.
7 Y. Sakamoto, S. Inomata and J. Hirokawa, *J. Phys. Chem. A*, 2013, **117**, 12912–12921.
8 R. L. Mauldin, T. Berndt, M. Sipila, P. Paasonen, T. Petaja, S. Kim, T. Kurten, F. Stratmann, V. M. Kerminen and M. Kulmala, *Nature*, 2012, **488**, 193–196.
9 M. Beck, R. Winterhalter, F. Herrmann and G. K. Moortgat, *Phys. Chem. Chem. Phys.*, 2011, **13**, 10970–11001.
10 R. Winterhalter, F. Herrmann, B. Kanawati, T. L. Nguyen, J. Peeters, L. Vereecken and G. K. Moortgat, *Phys. Chem. Chem. Phys.*, 2009, **11**, 4152–4172.
11 H. L. Huang, W. Chao and J. J. M. Lin, *Proc. Natl. Acad. Sci. U. S. A.*, 2015, **112**, 10857–10862.
12 K. Matsuoka, Y. Sakamoto, T. Hama, Y. Kajii and S. Enami, *J. Phys. Chem. A*, 2017, **121**, 810–818.
13 S. Enami, H. Mishra, M. R. Hoffmann and A. J. Colussi, *J. Phys. Chem. A*, 2012, **116**, 6027–6032.
14 S. Enami, M. R. Hoffmann and A. J. Colussi, *J. Phys. Chem. Lett.*, 2012, **3**, 3102–3108.
15 J. Liggio, S. M. Li, J. R. Brook and C. Mihele, *Geophys. Res. Lett.*, 2007, **34**, 28468.
16 B. M. Connelly and M. A. Tolbert, *Environ. Sci. Technol.*, 2010, **44**, 4603–4608.
17 F. Spielmann, S. Langebner, A. Ghirardo, A. Hansel, J. P. Schnitzler and G. Wohlfahrt, *Plant Soil*, 2017, **410**, 313–322.
18 E. Potier, B. Loubet, B. Durand, D. Flura, M. Bourdat-Deschamps, R. Ciuraru and J. Ogée, *Atmos. Environ.*, 2017, **151**, 176–187.
19 S. Enami, M. R. Hoffmann and A. J. Colussi, *J. Phys. Chem. Lett.*, 2010, **1**, 2374–2379.
20 C. Q. Zhu, M. Kumar, J. Zhong, L. Li, J. S. Francisco and X. C. Zeng, *J. Am. Chem. Soc.*, 2016, **138**, 11164–11169.
21 S. Enami and A. J. Colussi, *J. Phys. Chem. Lett.*, 2017, **8**, 1615–1623.
22 T. Hede, X. Li, C. Leck, Y. Tu and H. Ågren, *Atmos. Chem. Phys.*, 2011, **11**, 6549–6557.
23 S. Hatakeyama, K. Izumi, T. Fukuyama and H. Akimoto, *J. Geophys. Res.: Atmos.*, 1989, **94**, 13013–13024.
24 J. H. Seinfeld and S. N. Pandis, *Atmospheric chemistry and physics: from air pollution to climate change*, Wiley, Hoboken, N.J., 2nd edn, 2006.
25 I. G. Kavouras, N. Mihalopoulos and E. G. Stephanou, *Nature*, 1998, **395**, 683–686.
26 S. Lee and R. M. Kamens, *Atmos. Environ.*, 2005, **39**, 6822–6832.
27 K. E. Daumit, A. J. Carrasquillo, R. A. Sugrue and J. H. Kroll, *J. Phys. Chem. A*, 2016, **120**, 1386–1394.
28 H. Lignell, S. A. Epstein, M. R. Marvin, D. Shemesh, R. B. Gerber and S. Nizkorodov, *J. Phys. Chem. A*, 2013, **117**, 12930–12945.
29 C. D. O'Dowd, P. Aalto, K. Hameri, M. Kulmala and T. Hoffmann, *Nature*, 2002, **416**, 497–498.
30 P. Q. Fu, K. Kawamura, Y. Kanaya and Z. F. Wang, *Atmos. Environ.*, 2010, **44**, 4817–4826.
31 Y. Y. Zhang, L. Muller, R. Winterhalter, G. K. Moortgat, T. Hoffmann and U. Poschl, *Atmos. Chem. Phys.*, 2010, **10**, 7859–7873.
32 I. G. Kavouras, N. Mihalopoulos and E. G. Stephanou, *Environ. Sci. Technol.*, 1999, **33**, 1028–1037.
33 X. Li, T. Hede, T. Tu, C. Leck and H. Agren, *J. Phys. Chem. Lett.*, 2010, **1**, 769–773.
34 A. R. Hyvarinen, H. Lihavainen, A. Gaman, L. Vairila, H. Ojala, M. Kulmala and Y. Viisanen, *J. Chem. Eng. Data*, 2006, **51**, 255–260.
35 M. L. Shulman, M. C. Jacobson, R. J. Carlson, R. E. Synovec and T. E. Young, *Geophys. Res. Lett.*, 1996, **23**, 277–280.
36 R. Tuckermann, *Atmos. Environ.*, 2007, **41**, 6265–6275.
37 S. Enami and Y. Sakamoto, *J. Phys. Chem. A*, 2016, **120**, 3578–3587.
38 S. Enami and A. J. Colussi, *J. Phys. Chem. B*, 2013, **117**, 6276–6281.
39 S. Enami, T. Fujii, Y. Sakamoto, T. Hama and Y. Kajii, *J. Phys. Chem. A*, 2016, **120**, 9224–9234.
40 S. Enami, M. R. Hoffmann and A. J. Colussi, *J. Phys. Chem. Lett.*, 2010, **1**, 1599–1604.
41 K. A. Perrine, M. H. Van Spyk, A. M. Margarella, B. Winter, M. Faubel, H. Bluhm and J. C. Hemminger, *J. Phys. Chem. C*, 2014, **118**, 29378–29388.
42 M. J. Makowski, A. C. Stern, J. C. Hemminger and D. J. Tobias, *J. Phys. Chem. C*, 2016, **120**, 17555–17563.
43 S. Enami, Y. Sakamoto and A. J. Colussi, *Proc. Natl. Acad. Sci. U. S. A.*, 2014, **111**, 623–628.
44 S. Enami, M. R. Hoffmann and A. J. Colussi, *Phys. Chem. Chem. Phys.*, 2016, **18**, 31505–31512.
45 S. Enami, M. R. Hoffmann and A. J. Colussi, *J. Phys. Chem. A*, 2014, **118**, 4130–4137.
46 S. Enami and A. J. Colussi, *J. Chem. Phys.*, 2013, **138**, 184706.
47 J. Hoigne, H. Bader, W. R. Haag and J. Staehelin, *Water Res.*, 1985, **19**, 993–1004.
48 S. Enami, C. D. Vecitis, J. Cheng, M. R. Hoffmann and A. J. Colussi, *J. Phys. Chem. A*, 2007, **111**, 8749–8752.

49 A. J. Ingram, C. L. Boeser and R. N. Zare, *Chem. Sci.*, 2016, **7**, 39–55.
50 J. Laskin, A. Laskin and S. A. Nizkorodov, *Int. Rev. Phys. Chem.*, 2013, **32**, 128–170.
51 H. Howell and G. S. Fisher, *J. Am. Chem. Soc.*, 1958, **80**, 6316–6319.
52 J. W. Larson and T. B. McMahon, *J. Am. Chem. Soc.*, 1985, **107**, 766–773.
53 H. Bohringer, D. W. Fahey, F. C. Fehsenfeld and E. E. Ferguson, *J. Chem. Phys.*, 1984, **81**, 2805–2810.
54 M. Ghalaieny, A. Bacak, M. McGillen, D. Martin, A. V. Knights, S. O'Doherty, D. E. Shallcross and C. J. Percival, *Phys. Chem. Chem. Phys.*, 2012, **14**, 6596–6602.
55 C. R. Ruehl and K. R. Wilson, *J. Phys. Chem. A*, 2014, **118**, 3952–3966.
56 L. Müller, M. C. Reinnig, K. H. Naumann, H. Saathoff, T. F. Mentel, N. M. Donahue and T. Hoffmann, *Atmos. Chem. Phys.*, 2012, **12**, 1483–1496.
57 Y. Cheng, J. R. Brook, S. M. Li and A. Leithead, *Atmos. Environ.*, 2011, **45**, 7105–7112.
58 B. Witkowski and T. Gierczak, *J. Mass Spectrom.*, 2013, **48**, 79–88.
59 M. Y. Wang, L. Yao, J. Zheng, X. K. Wang, J. M. Chen, X. Yang, D. R. Worsnop, N. M. Donahue and L. Wang, *Environ. Sci. Technol.*, 2016, **50**, 5702–5710.
60 B. Witkowski and T. Gierczak, *Atmos. Environ.*, 2014, **95**, 59–70.
61 M. Sipilä, T. Jokinen, T. Berndt, S. Richters, R. Makkonen, N. M. Donahue, R. L. Mauldin Iii, T. Kurtén, P. Paasonen, N. Sarnela, M. Ehn, H. Junninen, M. P. Rissanen, J. Thornton, F. Stratmann, H. Herrmann, D. R. Worsnop, M. Kulmala, V. M. Kerminen and T. Petäjä, *Atmos. Chem. Phys.*, 2014, **14**, 12143–12153.
62 M. Ehn, J. A. Thornton, E. Kleist, M. Sipila, H. Junninen, I. Pullinen, M. Springer, F. Rubach, R. Tillmann, B. Lee, F. Lopez-Hilfiker, S. Andres, I. H. Acir, M. Rissanen, T. Jokinen, S. Schobesberger, J. Kangasluoma, J. Kontkanen, T. Nieminen, T. Kurten, L. B. Nielsen, S. Jorgensen, H. G. Kjaergaard, M. Canagaratna, M. Dal Maso, T. Berndt, T. Petaja, A. Wahner, V. M. Kerminen, M. Kulmala, D. R. Worsnop, J. Wildt and T. F. Mentel, *Nature*, 2014, **506**, 476–479.
63 K. Kristensen, Å. K. Watne, J. Hammes, A. Lutz, T. Petäjä, M. Hallquist, M. Bilde and M. Glasius, *Environ. Sci. Technol. Lett.*, 2016, **3**, 280–285.
64 H. Tong, A. M. Arangio, P. S. J. Lakey, T. Berkemeier, F. Liu, C. J. Kampf, W. H. Brune, U. Pöschl and M. Shiraiwa, *Atmos. Chem. Phys.*, 2016, **16**, 1761–1771.
65 E. Vidrio, C. H. Phuah, A. M. Dillner and C. Anastasio, *Environ. Sci. Technol.*, 2009, **43**, 922–927.
66 L. Vereecken, H. Harder and A. Novelli, *Phys. Chem. Chem. Phys.*, 2014, **16**, 4039–4049.
67 H. G. Kjaergaard, T. Kurten, L. B. Nielsen, S. Jorgensen and P. O. Wennberg, *J. Phys. Chem. Lett.*, 2013, **4**, 2525–2529.
68 A. Rouviere and M. Ammann, *Atmos. Chem. Phys.*, 2010, **10**, 11489–11500.
69 S. C. Park, D. K. Burden and G. M. Nathanson, *Acc. Chem. Res.*, 2009, **42**, 379–387.
70 T. Kinugawa, S. Enami, A. Yabushita, M. Kawasaki, M. R. Hoffmann and A. J. Colussi, *Phys. Chem. Chem. Phys.*, 2011, **13**, 5144–5149.
71 S. Enami, M. R. Hoffmann and A. J. Colussi, *J. Phys. Chem. A*, 2010, **114**, 5817–5822.
72 D. J. Donaldson and K. T. Valsaraj, *Environ. Sci. Technol.*, 2010, **44**, 865–873.
73 J. P. Reid, B. J. Dennis-Smither, N.-O. A. Kwamena, R. E. Miles, K. L. Hanford and C. J. Homer, *Phys. Chem. Chem. Phys.*, 2011, **13**, 15559–15572.
74 J. A. Faust, J. P. Wong, A. K. Lee and J. P. Abbatt, *Environ. Sci. Technol.*, 2017, **51**, 1405–1413.
75 O. Welz, A. J. Eskola, L. Sheps, B. Rotavera, J. D. Savee, A. M. Scheer, D. L. Osborn, D. Lowe, A. M. Booth, P. Xiao, M. A. H. Khan, C. J. Percival, D. E. Shallcross and C. A. Taatjes, *Angew. Chem., Int. Ed.*, 2014, **53**, 4547–4550.
76 M. Riva, S. H. Budisulistiorini, Z. Zhang, A. Gold, J. A. Thornton, B. J. Turpin and J. D. Surratt, *Atmos. Environ.*, 2017, **152**, 314–322.
77 K. C. Barsanti, J. H. Kroll and J. A. Thornton, *J. Phys. Chem. Lett.*, 2017, **8**, 1503–1511.
78 F. Riccobono, S. Schobesberger, C. E. Scott, J. Dommen, I. K. Ortega, L. Rondo, J. Almeida, A. Amorim, F. Bianchi, M. Breitenlechner, A. David, A. Downard, E. M. Dunne, J. Duplissy, S. Ehrhart, R. C. Flagan, A. Franchin, A. Hansel, H. Junninen, M. Kajos, H. Keskinen, A. Kupc, A. Kurten, A. N. Kvashin, A. Laaksonen, K. Lehtipalo, V. Makhmutov, S. Mathot, T. Nieminen, A. Onnela, T. Petaja, A. P. Praplan, F. D. Santos, S. Schallhart, J. H. Seinfeld, M. Sipila, D. V. Spracklen, Y. Stozhkov, F. Stratmann, A. Tome, G. Tsagkogeorgas, P. Vaattovaara, Y. Viisanen, A. Vrtala, P. E. Wagner, E. Weingartner, H. Wex, D. Wimmer, K. S. Carslaw, J. Curtius, N. M. Donahue, J. Kirkby, M. Kulmala, D. R. Worsnop and U. Baltensperger, *Science*, 2014, **344**, 717–721.
79 A. H. Goldstein and I. E. Galbally, *Environ. Sci. Technol.*, 2007, **41**, 1514–1521.